Predicting Boron Adsorption by Soils Using Soil Chemical Parameters in the Constant Capacitance Model

Sabine Goldberg,* Scott M. Lesch, and Donald L. Suarez

ABSTRACT

The constant capacitance model, a chemical surface complexation model, was applied to B adsorption on 17 soils selected for variation in soil properties. A general regression model was developed for predicting soil B surface complexation constants from easily measured soil chemical characteristics. These chemical properties were cation-exchange capacity (CEC), surface area, organic carbon content (OC), and inorganic carbon content (IOC). The prediction equations were used to obtain values for B surface complexation constants for 15 additional soils, thereby providing a completely independent evaluation of the ability of the constant capacitance model to fit B adsorption. The model was well able to predict B adsorption on the 15 soils. Incorporation of these prediction equations into chemical speciation–transport models will allow simulation of soil solution B concentrations under diverse environmental and agricultural conditions without the requirement of soil specific adsorption data and subsequent parameter optimization.

Boron is both a micronutrient essential for plant growth and a potentially toxic trace element. The range between B deficiency and toxicity symptoms in plants is narrow typically in the range of 0.028 to 0.093 mmol L^{-1} for sensitive crops and 0.37 to 1.39 mmol L^{-1} for tolerant crops (Keren and Bingham, 1985). Excess soil solution B concentrations can lead to marked yield decrement in crop plants resulting in economic losses. For this reason, careful quantification of soil solution B concentrations is needed, especially in regions such as the southwestern USA where B toxicity often limits full use of water resources. Adsorption of B on soil mineral surfaces is important to managing B toxicity or deficiency since adsorbed B is not perceived as toxic by plants (Keren et al., 1985).

Availability of B to plants is affected by a variety of factors including soil solution pH, soil texture, soil moisture, temperature, oxide content, carbonate content, organic matter content, and clay mineralogy (Keren and Bingham, 1985). Boron becomes less available with increasing solution pH. Boron deficiency often occurs on sandy soils and during hot, dry soil conditions. The dominant B adsorbing surfaces in soil are oxides, clay minerals, calcite, and organic matter (Goldberg, 1993).

Boron adsorption on soils and soil minerals has been described using various modeling approaches. Such models include the empirical Freundlich and Langmuir adsorption isotherms (Elrashidi and O'Connor, 1982; Goldberg and Forster, 1991) and surface complexation models: constant capacitance model (Goldberg and Glaubig, 1985, 1986a, 1986b, 1988; Goldberg et al., 1993), triple layer model (Singh and Mattigod, 1992; Toner and Sparks, 1995), and Stern variable surface charge–variable surface potential model (Bloesch et al., 1987). Parameters from empirical models are only valid for the particular conditions of the experiment. Surface complexation models are chemical models that use defined surface species, chemical reactions, mass balances, and charge balance. They contain molecular features that can be given thermodynamic significance (Sposito, 1983).

Chemical modeling of B adsorption at the mineral–solution interface has been successful using the constant capacitance model for oxides, clay minerals, and soils (Goldberg and Glaubig, 1985, 1986a, 1986b, 1988, Goldberg et al., 1993). In these studies B adsorption was described as forming a trigonal inner-sphere surface complex. Such a configuration is chemically reasonable since boric acid is a very weak monobasic acid with a pK_a of 9.2 and thus trigonal over most of the pH range. Although it is reasonable for the dominant solution species to be dominant on the exchange complex, there is no 1:1 correspondence between solution and surface species (Sposito, 1983). Boric acid acts as a Lewis acid by accepting a hydroxyl ion to form the tetrahedral borate anion:

$$H_3BO_3 + H_2O \rightleftharpoons B(OH)_4^- + H^+ \quad [1]$$

Recent research using Attenuated Total Reflectance Fourier Transform Infrared Spectroscopy has provided direct evidence for the presence of tetrahedral B as well as trigonal B adsorbed on the surface of amorphous Al hydroxide (Su and Suarez, 1995). Their study was carried out under aqueous conditions so the results are directly applicable to natural soil systems. Spectroscopic investigations of B adsorbed to organic matter and carbonates have not yet been carried out. Boron adsorption on arid zone soils was successfully described with the constant capacitance model using both trigonal and tetrahedral B surface configurations consistent with microscopic experimental results (Goldberg, 1999). The study of Goldberg (1999) fit the constant capacitance model to each of 14 soil samples and tested the ability of an average set of B surface complexation constants to predict B adsorption.

The objectives of the present study are (i) to apply the constant capacitance model to B adsorption on an expanded set of 32 soil samples using both trigonal and tetrahedral surface configurations for adsorbed B; (ii) to relate B adsorption characteristics and model surface complexation constants to easily measured chemical pa-

USDA-ARS, George E. Brown, Jr., Salinity Laboratory, 450 W. Big Springs Road, Riverside, CA 92507. Contribution from the George E. Brown, Jr., Salinity Lab. Received 6 Sept. 1999. *Corresponding author (sgoldberg@ussl.ars.usda.gov).

Published in Soil Sci. Soc. Am. J. 64:1356–1363 (2000).

Abbreviations: CEC, cation-exchange capacity; IOC, inorganic carbon content; OC, organic carbon content; SA, surface area; %Al, mass percent aluminum oxide; %Fe, mass percent iron oxide content.

Table 1. Classifications and chemical characteristics of soils†.

Soil series	Depth	CEC	SA	IOC	OC	Fe	Al
	cm	$mmol_c\ kg^{-1}$	$m^2\ kg^{-1}$	$g\ kg^{-1}$			
Altamont (fine, smectitic, thermic Aridic Haploxerert)	0–25	152	0.103	0.0099	9.6	7.7	0.58
	25–51	160	0.114	0.011	6.7	8.2	0.64
	0–23	179	0.109	0.12	30.8	9.2	0.88
Arlington (coarse-loamy, mixed thermic Haplic Durixeralf)	0–25	107	0.0611	0.30	4.7	8.2	0.48
	25–51	190	0.103	0.16	2.8	10.1	0.60
Bonsall (fine, smectitic, thermic Natric Palexeralf)	0–25	54	0.0329	0.13	4.9	9.3	0.45
	25–51	122	0.106	0.07	2.1	16.8	0.91
Fallbrook (fine-loamy, mixed, thermic Typic Haploxeralf)	0–25	112	0.0683	0.023	3.5	6.9	0.36
	25–51	78	0.0285	0.24	3.1	4.9	0.21
Imperial (fine, smectitic, calcareous, hyperthermic Vertic Torrifluvent)	Surface	222	0.196	18.6	9.1	6.1	0.38
	0–7.6	229	0.191	17.6	8.3	6.7	0.43
	15–46	198	0.106	17.9	4.5	7.0	0.53
Pachappa (coarse-loamy, mixed, thermic Mollic Haploxeralf)	0–25	39	0.0363	0.026	3.8	7.6	0.67
	25–51	52	0.041	0.014	1.1	7.2	0.35
Ramona (fine-loamy, mixed, thermic Typic Haploxeralf)	0–25	66	0.0279	0.02	4.4	4.5	0.42
	25–51	29	0.0388	0.018	2.2	5.9	0.40
Holtville (clayey over loamy, smectitic, mixed, calcareous, hyperthermic Typic Torrifluvent)	61–76	58	0.043	16.4	2.1	4.9	0.27
Haines (coarse-silty, mixed, calcareous, mesic Typic Haplaquept)	20	80	0.0595	15.8	14.9	1.7	0.18
Diablo (fine, smectitic, thermic Aridic Haploxerert)	0–15	301	0.19	0.26	19.8	7.1	1.02
	0–15	234	0.13	2.2	28.3	5.8	0.84
Sebree (fine-silty, mixed, mesic Xerollic Nadurargid)	0–13	27	0.0212	0.0063	2.2	6.0	0.46
Ryepatch (very-fine, smectitic, calcareous, mesic Vertic Endoaquoll)	0–15	385	0.213	2.5	32.4	2.6	0.92
Hanford (coarse-loamy, mixed, nonacid, thermic Typic Xerorthent)	0–10	111	0.0289	10.1	28.7	6.6	0.35
Avon (fine, smectitic, mesic, calcic Pachic Argixeroll)	0–15	183	0.0601	0.083	30.8	4.3	0.78
Reagan (fine-silty, mixed, thermic Ustic Haplocalcid)	Surface	98	0.0588	18.3	10.1	4.6	0.45
Fiander (fine-silty, mixed, mesic Typic Natraquoll)	0–15	248	0.0925	6.9	4.0	9.2	1.06
Yolo (fine-silty, mixed, nonacid, thermic Typic Xerorthent)	0–15	177	0.0730	0.23	11.5	15.6	1.13
Nohili (very-fine, smectitic, calcareous, isohyperthermic Cumulic Endoaquoll)	0–23	467	0.286	2.7	21.3	49.0	3.7
Porterville (fine, smectitic, thermic Aridic Haploxerert)	0–7.6	203	0.172	0.039	9.4	10.7	0.90
Hesperia (coarse-loamy, mixed, nonacid, thermic Xeric Torriorthent)	0–7.6	45	0.0309	0.018	4.9	3.2	0.34
Wasco (coarse-loamy, mixed, nonacid, thermic Typic Torriorthent)	0–5.1	71	0.0559	0.009	4.7	2.4	0.42
Wyo (fine-loamy, mixed, thermic Mollic Haploxeralf)		155	0.0782	0.014	19.9	9.5	0.89

† CEC, cation-exchange capacity; SA, surface area; IOC, inorganic carbon content; OC, organic carbon content.

rameters affecting B adsorption, such as surface area (SA), CEC, OC, IOC, mass percent aluminum (%Al) oxide, and mass percent iron (%Fe) oxide content; (iii) to quantitatively relate variations in these soil properties to variations in values of surface complexation constants obtained with the constant capacitance model; and (iv) to evaluate the ability of the constant capacitance model to predict B adsorption on additional soils using the surface complexation constants calculated from soil chemical properties.

MATERIALS AND METHODS

Boron adsorption was investigated using 32 surface and subsurface soil samples from 22 soil series belonging to six different soil orders. Boron adsorption on 14 of these soil samples had been determined previously by Goldberg and Glaubig (1986b); the remaining 18 soils used in the B adsorption experiment were chosen to provide a wider range of soil chemical characteristics. Soil classifications and chemical characteristics are given in Table 1.

Cation-exchange capacities were determined with the method for arid-zone soils described by Rhoades (1982). Surface areas were measured using ethylene glycol monoethyl ether (EGME) adsorption (Cihacek and Bremner, 1979). Free Fe and Al oxides were extracted according to the method of Coffin (1963). Aluminum and Fe concentrations in the extracts were determined by inductively coupled plasma (ICP) emission spectrometry. Organic and inorganic carbon were determined using a UIC Full Carbon System 150 with a C coulometer[1]. Total carbon was determined by furnace combustion at 950°C; IOC was determined using an acidification module and heating. Organic C was determined by difference.

Boron adsorption experiments were carried out in batch systems to determine adsorption envelopes, amount of B adsorbed as a function of solution pH per fixed total B concentration. Five grams of soil were added to 50-mL polypropylene centrifuge tubes and equilibrated with 25 mL of a 0.1 *M* NaCl solution by shaking for 20 h on a reciprocating shaker. This solution contained 0.463 mmol L^{-1} B and had been adjusted to the desired pH range of 3 to 10 using 1 M HCl or 1 *M* NaOH. Additions of acid or base changed the total volumes by <2%. After reaction, the samples were centrifuged and the decantates analyzed for pH, filtered and analyzed for B concentration using ICP emission spectrometry.

[1] Trade names and company names are included for the benefit of the reader and do not imply any endorsement or preferential treatment of the product listed by the U.S. Department of Agriculture.

A detailed discussion of the theory and assumptions of the constant capacitance model is provided in Goldberg (1992). In the present application of the constant capacitance model to B adsorption, the following surface complexation reactions were considered:

$$SOH_{(s)} + H^+_{(aq)} \rightleftharpoons SOH^+_{2(s)} \quad [2]$$

$$SOH_{(s)} \rightleftharpoons SO^-_{(s)} + H^+_{(aq)} \quad [3]$$

$$SOH_{(s)} + H_3BO_{3(aq)} \rightleftharpoons SH_2BO_{3(s)} + H_2O \quad [4]$$

$$SOH_{(s)} + H_3BO_{3(aq)} \rightleftharpoons SH_3BO^-_{4(s)} + H^+_{(aq)} \quad [5]$$

where SOH represents reactive surface hydroxyl groups on oxides and clay minerals in the soil. Both trigonal and tetrahedral B surface species were included, consistent with the experimental spectroscopic results of Su and Suarez (1995).

Intrinsic equilibrium constant expressions for the surface complexation reactions are

$$K_+(\text{int}) = \frac{[SOH^+_2]}{[SOH][H^+]} \exp(F\psi/RT) \quad [6]$$

$$K_-(\text{int}) = \frac{[SO^-][H^+]}{[SOH]} \exp(-F\psi RT) \quad [7]$$

$$K_B(\text{int}) = \frac{[SH_2BO_3]}{[SOH][H_3BO_3]} \quad [8]$$

$$K_{B-}(\text{int}) = \frac{[SH_3BO^-_4][H^+]}{[SOH][H_3BO_3]} \exp(-F\psi RT) \quad [9]$$

where F is the Faraday constant (C mol_c^{-1}), ψ is the surface potential (V), R is the molar gas constant (J mol^{-1} K^{-1}), T is the absolute temperature (K), and square brackets indicate concentrations (mol L^{-1}). The exponential terms can be considered as solid-phase activity coefficients correcting for the charges on the surface complexes.

Mass balance for the reactive surface functional group is

$$[SOH]_T = [SOH] + [SOH^+_2] + [SO^-] + [SH_2BO_3] + [SH_3BO^-_4] \quad [10]$$

Charge balance is

$$\sigma = [SOH^+_2] - [SO^-] - [SH_3BO^-_4] \quad [11]$$

where σ has units of mol L^{-1}.

The computer program FITEQL 3.2 (Herbelin and Westall, 1996) was used to fit B surface complexation constants to the experimental B adsorption data. FITEQL 3.2 uses a nonlinear least squares optimization routine to fit equilibrium constants to experimental data. The FITEQL program contains the constant capacitance model of adsorption and can also be used as a chemical speciation model to evaluate predictions using previously determined equilibrium constants.

Initial input parameter values for the constant capacitance model were capacitance: C = 1.06 F m^{-2} (considered optimum for Al oxide by Westall and Hohl, 1980); protonation constant: log K_+ = 7.35; dissociation constant: log K_- = −8.95 (averages of a literature compilation for Al and Fe oxides from Goldberg and Sposito, 1984). A previous sensitivity analysis showed that capacitance changes in the range of 1.06 to 4.52 F m^{-2} produced minor changes in the values of the surface complexation constants (Goldberg and Sposito, 1984). Protonation–dissociation constant values for the constant capacitance model are not available for organic matter. To describe charging of carbonates six reactions are needed. For these reasons protonation–dissociation constants for Al and Fe oxides were chosen as starting values. These parameters were optimized in subsequent modeling. The total number of reactive surface hydroxyl groups, $[SOH]_T$, was set to a site density of 2.31 sites nm^{-2} as had been recommended for natural materials by Davis and Kent (1990). Surface complexation modeling of B adsorption is sensitively dependent on surface site density (Goldberg, 1991). For this reason it is critical to choose a consistent value of surface site density for incorporation into chemical speciation–transport models. Constant values of capacitance and site density are necessary to allow application of prediction equations to new soils.

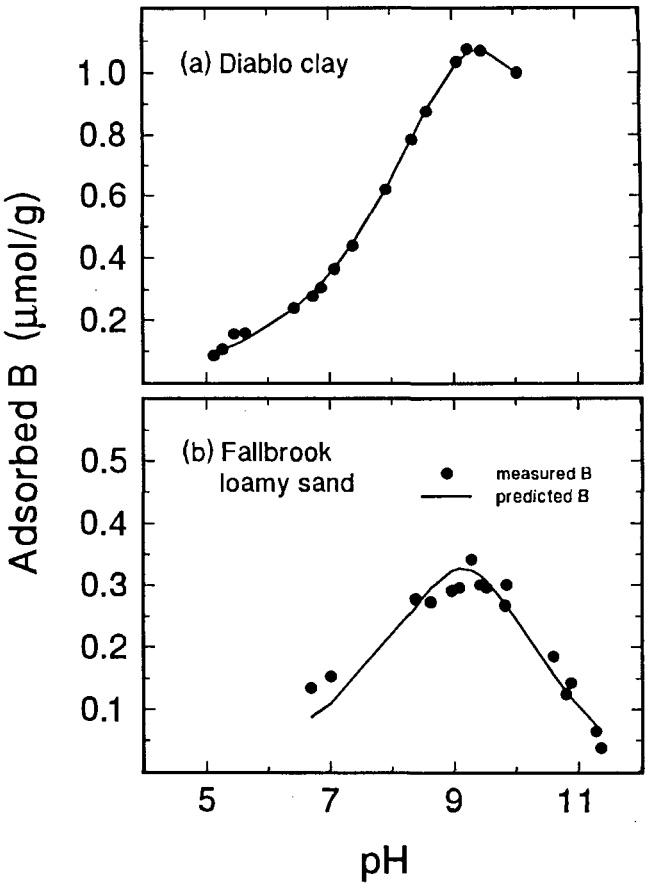

Fig. 1. Fit of the constant capacitance model to B adsorption: (a) Diablo clay; (b) Fallbrook loamy sand. Circles represent experimental data. Model fits are represented by solid lines. Fallbrook subsoil experimental data represented in Goldberg (1993).

RESULTS AND DISCUSSION

Boron adsorption as a function of solution pH was determined for 32 different arid zone soil samples (examples are presented in Fig. 1–3). Boron adsorption increases with increasing solution pH, exhibits a maximum adsorption around pH 9, and decreases with further increases in solution pH. This type of parabolic behavior is characteristic for B adsorption.

The constant capacitance model was fit to the B adsorption envelopes of all of the soil samples optimizing surface complexation constants for both the trigonal and the tetrahedral surface configurations of adsorbed B. Except for two soils, the model was unable to optimize values of the trigonal B constant, log K_B, since

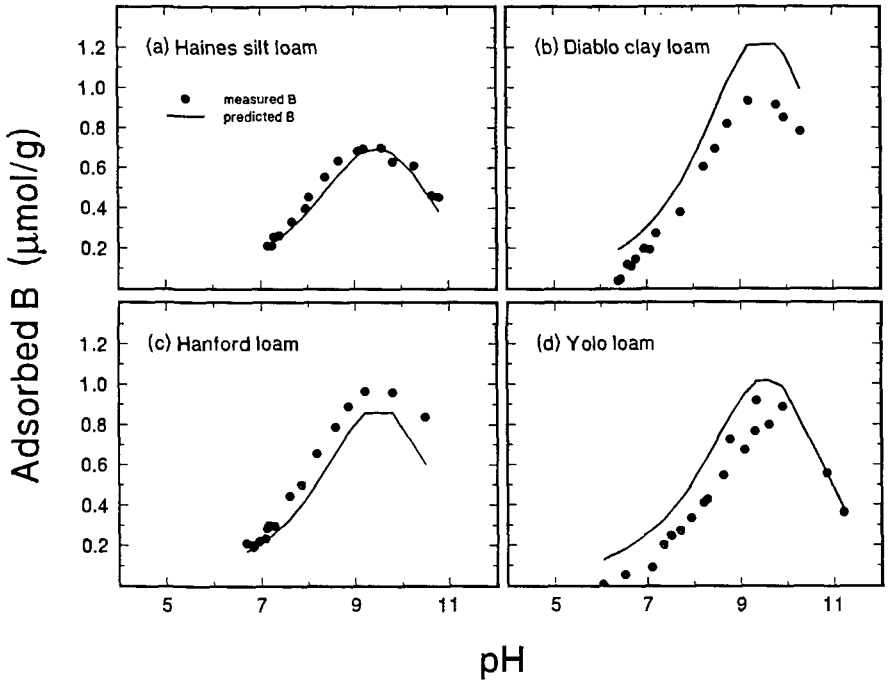

Fig. 2. Prediction of B adsorption with the constant capacitance model on soils used to obtain the prediction equations: (a) Haines silt loam; (b) Diablo clay loam; (c) Hanford loam; (d) Yolo loam. Circles represent experimental data. Model predictions are represented by solid lines.

the model optimization predicted that tetrahedral B dominated the adsorption complex. The model optimization does not see a statistically significant improvement in fit from including the trigonal B constant. To further improve the model fit, values of the protonation constant, log K_+, and the dissociation constant, log K_-, were simultaneously optimized with the tetrahedral B surface complexation constant, log K_{B-}. Simultaneous optimization was possible for only 17 out of 32 soil samples. Table 2 provides values of the simultaneously optimized surface complexation constants. Simultaneous optimization is considered statistically necessary for developing prediction equations because of the high degree of correlation of the three surface complexation constants. Figure 1 indicates the ability of the constant capacitance model to describe B adsorption on two soils by simultaneously optimizing $\log K_{B-}$(int), $\log K_+$(int), and $\log K_-$(int). In both cases the model provides a quantitative description of the adsorption data. Fits of similar quality were obtained for the remaining soils.

A general regression modeling approach was used to relate the chemical constants to the following set of soil chemical properties: CEC, SA, IOC, OC, %Fe, and %Al. Values for the correlation coefficients between

Table 2. Constant capacitance model surface complexation constants.

		Simultaneous optimization			From prediction equations		
Soil series	Depth	$\log K_{B-}$	$\log K_+$	$\log K_-$	$\log K_{B-}$	$\log K_+$	$\log K_-$
	cm						
Altamont loam	0–25	−8.88	9.44	−10.90	−8.67	8.87	−11.72
Arlington loam	0–25	−8.58	8.73	−12.55	−8.30	8.39	−11.79
	25–51	−8.36	7.99	−12.01	−8.55	8.43	−11.92
Bonsall clay loam	25–51	−8.44	8.75	−11.96	−8.51	8.36	−11.93
Fallbrook sandy loam	0–25	−8.62	8.82	−12.65	−8.82	9.11	−12.12
Fallbrook loamy sand	25–51	−8.52	8.81	−11.85	−8.50	8.99	−12.18
Imperial silty clay	Surface	−8.24	7.66	−11.38	−8.28	7.65	−11.42
Imperial silty clay	0–7.6	−8.15	7.52	−11.17	−8.24	7.59	−11.42
Imperial clay	15–46	−7.95	7.88	−11.35	−8.02	7.52	−11.54
Ramona sandy loam	25–51	−8.64	8.93	−12.10	−8.66	9.14	−12.24
Holtville sandy loam	61–76	−8.26	7.96	−11.75	−8.13	8.04	−11.98
Haines silt loam	20	−8.20	8.31	−11.82	−8.12	8.10	−11.51
Diablo clay	0–15	−8.33	8.12	−11.58	−8.15	7.80	−11.14
Diablo clay loam	0–15	−7.81	6.99	−10.52	−7.81	7.46	−10.97
Hanford loam	0–15	−7.38	7.70	−11.34	−7.48	7.71	−11.14
Avon silt loam	0–15	−7.65	8.06	−11.08	−7.90	8.15	−11.15
Yolo loam	0–15	−7.90	7.39	−11.38	−7.79	7.73	−11.24

Table 3. Correlation coefficients between variables†.

	CEC	SA	IOC	OC	Fe	Al
CEC	1.00	0.84**	0.06	0.40	0.14	0.56*
SA		1.00	0.27	0.07	0.12	0.31
IOC			1.00	−0.05	−0.39	−0.48
OC				1.00	−0.28	0.29
Fe					1.00	0.69**
Al						1.00

*, ** Significant at the 0.05 and 0.01 probability levels, respectively.
† CEC, cation-exchange capacity; SA, surface area; IOC, inorganic carbon content; OC, organic carbon content.

the soil chemical properties are given in Table 3 and indicate significant interactions between CEC and SA and between %Fe and %Al. In order to improve the empirical modeling process, we chose to limit the data fitting analysis to only those 17 soil samples whose surface complexation constants could be simultaneously optimized by the FITEQL program. The 17 soils used to obtain the regression model results discussed below had the following ranges of soil properties: CEC, 29 to 301 $mmol_c\ L^{-1}$; SA, 29 to 196 $m^2\ g^{-1}$; IOC, 0.001 to 1.9%; OC, 0.21 to 3.1%; Fe, 0.17 to 1.7%; and Al, 0.018 to 0.13%. This population of soils represented a wide range of soil chemical properties since each parameter varied by at least an order of magnitude. These 17 soils had the following ranges of fitted surface complexation constants: $\log K_{B-}(\text{int})$, −8.884 to −7.384; $\log K_{+}(\text{int})$, 7.388 to 9.443; and $\log K_{-}(\text{int})$, −12.55 to −10.52.

An exploratory data analysis revealed that all three of the model surface complexation constants appeared to be related to each of the log transformed chemical variables in at least a weakly linear manner. Therefore, the following initial regression model was specified for each of the chemical constants:

$$\gamma_i = b_{(0,i)} + b_{(1,i)}\ln(\text{CEC}) + b_{(2,i)}\ln(\text{SA}) + b_{(3,i)}\ln(\text{OC}) + b_{(4,i)}\ln(\text{IOC}) + b_{(5,i)}\ln(\%\text{Fe}) + b_{(6,i)}\ln(\%\text{Al}) + \varepsilon_i \quad [12]$$

where γ represents a specific, log transformed chemical constant, b_0 through b_6 represent empirical regression coefficients, and ε represents the stochastic random er-

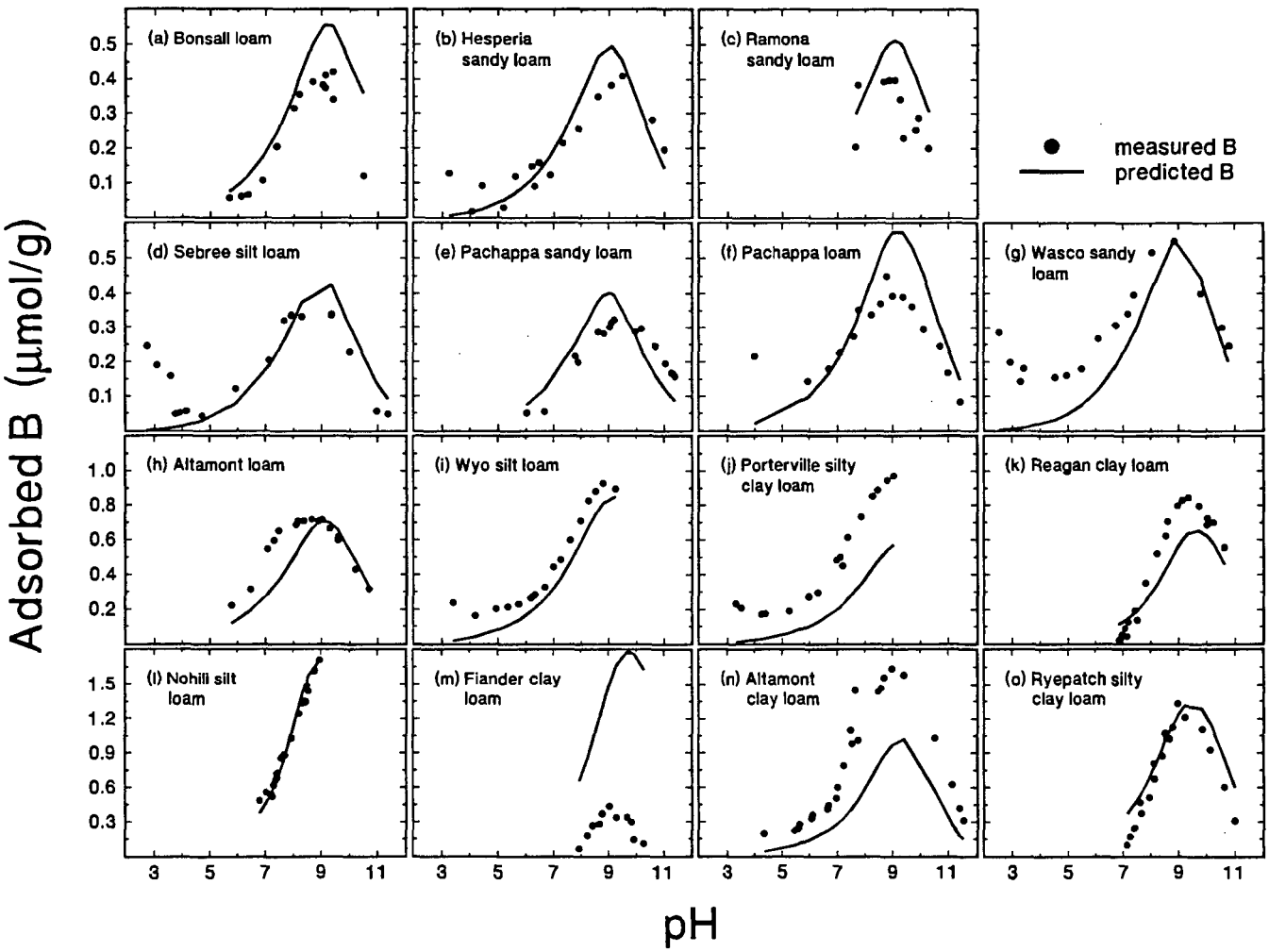

Fig. 3. Prediction of B adsorption with the constant capacitance model on soils not used to obtain the prediction equations: (a) Bonsall loam; (b) Hesperia sandy loam; (c) Ramona sandy loam; (d) Sebree silt loam; (e) Pachappa sandy loam; (f) Pachappa loam; (g) Wasco sandy loam; (h) Altamont loam; (i) Wyo silt loam; (j) Porterville silty clay loam; (k) Reagan clay loam; (l) Nohili silt loam; (m) Fiander clay loam; (n) Altamont clay loam; (o) Ryepatch silty clay loam. Circles represent experimental data. Model predictions are represented by solid lines. Altamont soil experimental data represented in Goldberg and Glaubig (1986b); Bonsall soil experimental data represented in Goldberg (1986).

ror component. Neither the CEC nor Fe chemical variables were found to be statistically significant after fitting Eq. [12] to each set of surface complexation constants. Additionally, the SA variable was not found to be significantly related to either the $\log K_+$ or $\log K_-$ constants, after accounting for the remaining variables. Hence, for the $\log K_{B-}$ constant, Eq. [12] was reduced to

$$\gamma_1 = b_{(0,1)} + b_{(2,1)}\ln(SA) + b_{(3,1)}\ln(OC) + b_{(4,1)}\ln(IOC) + b_{(6,1)}\ln(\%Al) + \varepsilon_1 \quad [13]$$

Likewise, Eq. [12] was reduced to

$$\gamma_2 = b_{(0,2)} + b_{(3,2)}\ln(OC) + b_{(4,2)}\ln(IOC) + b_{(6,2)}\ln(\%Al) + \varepsilon_2 \quad [14]$$

$$\gamma_3 = b_{(0,3)} + b_{(3,3)}\ln(OC) + b_{(4,3)}\ln(IOC) + b_{(6,3)}\ln(\%Al) + \varepsilon_3 \quad [15]$$

for the $\log K_+$ and $\log K_-$ constants, respectively. Table 4 provides parameter values for Eq. [13], [14], and [15]. It is chemically reasonable that the B surface complexation constant value is related to surface area, organic carbon, inorganic carbon, and Al oxide content since these soil properties have been found previously to be correlated with B adsorption (Goldberg, 1993).

A comprehensive residual analysis was performed on the regression model errors from Eq. [13], [14], and [15]; no regression modeling violations or data outliers were detected. Additionally, all the chemical variables in Eq. [13] were found to be statistically significant below the 0.01 level, and all of the variables remaining in Eq. [14] and [15] were statistically significant below the 0.05 level in at least one of the two ($\log K_+$ and $\log K_-$) surface complexation constant regression models. Table 4 displays the final parameter estimates, standard errors, and summary statistics for each of these regression models.

The prediction equations were used to obtain values of the surface complexation constants for the 17 soils used to obtain the general regression model (see Table 2). Since these soils had been used to obtain the prediction equations such an evaluation is not an independent assessment of predictive ability. Nevertheless, it is worthwhile to examine the quality of such predictions since they would be expected to be good. Figure 2 presents the ability of the constant capacitance model to predict B adsorption from chemical properties for four of the soils used to obtain the prediction equations. Figure 2a presents the best prediction, a quantitative representation of the experimental data (three other soils were found to be predicted this well). Figure 2b shows the worst prediction (one other soil was found to be predicted this poorly). Despite the overprediction especially near the adsorption maximum, the model reproduced the shape of the adsorption envelope. Figures 2c and 2d present typical underprediction (five soils were predicted similarly) and overprediction (four soils were predicted similarly) of experimental data. In general, the constant capacitance model is well able to de-

Table 5. Constant capacitance model surface complexation constants.

Soil series	Depth	From prediction equations		
		$\log K_{B-}$	$\log K_+$	$\log K_-$
	cm			
Altamont loam	25–21	−8.71	8.83	−11.79
Altamont clay loam	0–23	−8.03	8.00	−11.10
Bonsall loam	0–25	−8.19	8.59	−11.85
Pachappa loam	0–25	−8.26	8.69	−11.90
Pachappa sandy loam	25–51	−8.89	9.34	−12.50
Ramona sandy loam	0–25	−8.38	9.01	−12.01
Sebree silt loam	0–13	−8.48	9.26	−12.26
Ryepatch silty clay loam	0–15	−7.91	7.37	−10.89
Reagan clay loam	Surface	−7.73	7.54	−11.34
Fiander clay loam	0–15	−7.77	7.29	−11.42
Nohili silt loam	0–23	−7.43	6.53	−10.59
Porterville silty clay loam	0–7.6	−8.51	8.33	−11.51
Hesperia sandy loam	0–7.6	−8.52	9.16	−12.05
Wasco sandy loam	0–5.1	−8.72	9.17	−12.04
Wyo silt loam		−8.21	8.47	−11.35

Table 4. Regression model summary statistics, parameter estimates, and standard errors.

Constant	R^2	MSE	Model F score	Prob. > F
	Model summary statistics			
$\log K_{B-}$	0.858	0.02910	18.11	0.0001
$\log K_+$	0.768	0.12101	14.35	0.0002
$\log K_-$	0.528	0.18239	4.85	0.0177

Constant	Parameter	Parameter estimate	Parameter standard error	t score	Prob. > |t|
	Parameter estimates				
$\log K_{B-}$	intercept	−9.136	0.219	−41.63	0.0001
	ln(SA)	−0.375	0.087	−4.30	0.0010
	ln(OC)	0.167	0.050	3.36	0.0057
	ln(IOC)	0.111	0.020	5.61	0.0001
	ln(%Al)	0.466	0.112	4.17	0.0013
$\log K_+$	intercept	7.852	0.299	26.22	0.0001
	ln(OC)	−0.102	0.101	−1.01	0.3326
	ln(IOC)	−0.198	0.037	−5.35	0.0001
	ln(%Al)	−0.622	0.185	−3.37	0.0051
$\log K_-$	intercept	−11.967	0.368	−32.55	0.0001
	ln(OC)	0.302	0.124	2.43	0.0306
	ln(IOC)	0.058	0.045	1.29	0.2204
	ln(%Al)	0.302	0.227	1.33	0.2061

scribe B adsorption on the 17 soils used to obtain the prediction equations.

The prediction equations were also used to predict surface complexation constants for the remaining 15 soils that had not been used to obtain the general regression model (see Table 5). The constant capacitance model containing these surface complexation constants was then used to predict B adsorption on the 15 soils. Since the data from the 15 soils had not been used to develop the prediction equations, this represents an independent evaluation of their ability to predict B adsorption. Figure 3 indicates the ability of this approach to predict B adsorption on the 15 soils not used to obtain the prediction equations. For most of the soils the prediction of B adsorption is very reasonable (see Fig. 3a to 3h, 3k, 3l, 3o) The model always predicted the shape of the B adsorption envelopes. Figure 3l shows quantitative prediction of B adsorption for the Nohili soil. Interestingly, several of the chemical characteristics for this soil (CEC, SA, %Fe, and %Al) fell outside the range for the 17 soils used to obtain the prediction equations. This result suggests that the prediction equations may have applicability to other soils outside the present ranges of soil chemical characteristics. Figure 2m shows the worst prediction for any of the soils.

A forward stepwise linear regression model was also used to obtain alternative prediction equations. Variables were entered into the model if they met a 0.5 significance level. The stepwise prediction equations are

$$\log K_{B-} = -8.98 + 0.00351CEC - 0.00609SA + 0.263OC + 0.340IOC + 0.401Fe \quad [16]$$

$$\log K_{+} = 9.42 - 0.00495CEC + 0.00514SA - 0.132OC - 0.586IOC - 8.51Al \quad [17]$$

$$\log K_{-} = -12.51 + 0.00156SA + 0.312OC + 0.237IOC - 4.85Al \quad [18]$$

While the stepwise linear approach provided an improved prediction of the soils used to obtain the regression model, predictive capability for soils not used to develop the prediction equations suffered (data not shown). For this reason this approach was not pursued further.

While predictions of B adsorption for many of the soils are only semi-quantitative, these predictions were obtained independent of any experimental measurement of B adsorption on these soils using values of only a few easily measured chemical parameters which are more often available. Incorporation of these prediction equations into chemical speciation–transport models (such as UNSATCHEM; Suarez and Simunek, 1997), will allow simulation of B concentrations in soil solution under diverse environmental conditions. Future research will determine to what extent adequate simulations of B adsorption, release, and transport are possible using this approach without the necessity to perform time consuming detailed studies for each soil. Scenarios of agricultural and environmental interest include irrigation with high B waters and reclamation of high B soils.

ACKNOWLEDGMENTS

Gratitude is expressed to Mr. H.S. Forster, Mr. C. Bennett, Mr. D. Leang, and Ms. P. Takahashi for technical assistance, Dr. J.D. Rhoades for providing the soil samples, and Mr. S. Nakamura for providing the Nohili soil series classification.

REFERENCES

Bloesch, P.M., L.C. Bell, and J.D. Hughes. 1987. Adsorption and desorption of boron by goethite. Aust. J. Soil Res. 25:377–390.

Cihacek, L.J., and J.M. Bremner. 1979. A simplified ethylene glycol monoethyl ether procedure for assessing soil surface area. Soil Sci. Soc. Am. J. 43:821–822.

Coffin, D.E. 1963. A method for the determination of free iron oxide in soils and clays. Can. J. Soil Sci. 43:7–17.

Davis, J. A., and D.B. Kent. 1990. Surface complexation modeling in aqueous geochemistry. Rev. Mineral. 23:117–260.

Elrashidi, M.A., and G.A. O'Connor. 1982. Boron sorption and desorption in soils. Soil Sci. Soc. Am. J. 46:27–31.

Goldberg, S. 1986. Chemical modeling of specific anion adsorption on oxides, clay minerals, and soils. p. 671–688. *In* ENVIROSOFT 86. CML Publ., Ashurst, Southampton, UK.

Goldberg, S. 1991. Sensitivity of surface complexation modeling to the surface site density parameter. J. Colloid Interface Sci. 145:1–9.

Goldberg, S. 1992. Use of surface complexation models in soil chemical systems. Adv. Agron. 47:233–329.

Goldberg, S. 1993. Chemistry and mineralogy of boron in soils. p. 3–44. *In* Boron and its role in crop production. U.C. Gupta (ed.) CRC Press, Boca Raton, FL.

Goldberg, S. 1999. Reanalysis of boron adsorption on soils and soil minerals using the constant capacitance model. Soil Sci. Soc. Am. J. 63:823–829.

Goldberg, S., and H.S. Forster. 1991. Boron sorption on calcareous soils and reference calcites. Soil Sci. 152:304–310.

Goldberg, S., H.S. Forster, and E.L. Heick. 1993. Boron adsorption mechanisms on oxides, clay minerals, and soils inferred from ionic strength effects. Soil Sci. Soc. Am. J. 57:704–708.

Goldberg, S., and R.A. Glaubig. 1985. Boron adsorption on aluminum and iron oxide minerals. Soil Sci. Soc. Am. J. 49:1374–1379.

Goldberg, S., and R.A. Glaubig. 1986a. Boron adsorption and silicon release by the clay minerals kaolinite, montmorillonite, and illite. Soil Sci. Soc. Am. J. 50:1442–1448.

Goldberg, S., and R.A. Glaubig. 1986b. Boron adsorption on California soils. Soil Sci. Soc. Am. J. 50:1173–1176.

Goldberg, S., and R.A. Glaubig. 1988. Boron and silicon adsorption on an aluminum oxide. Soil Sci. Soc. Am. J. 52:87–91.

Goldberg, S., and Sposito, G. 1984. A chemical model of phosphate adsorption by soils: II. Noncalcareous soils. Soil Sci. Soc. Am. J. 48:779–783.

Herbelin, A.L., and J.C. Westall. 1996. FITEQL: A computer program for determination of chemical equilibrium constants from experimental data. Rep. 94-01, Version 3.2, Dep. of Chemistry, Oregon State Univ., Corvallis.

Keren, R., and F.T. Bingham. 1985. Boron in water, soils, and plants. Adv. Soil Sci. 1:229–276.

Keren, R., F.T. Bingham, and J.D. Rhoades. 1985. Plant uptake of boron as affected by boron distribution between liquid and solid phases in soil. Soil Sci. Soc. Am. J. 49:297–302.

Rhoades, J.D. 1982. Cation-exchange capacity. p. 149–157. *In* Methods of soil analysis. Part 2. 2nd ed. A.L. Page et al. (ed.) Agron. Monogr. 9. SSSA, Madison, WI.

Singh, P.N., and S.V. Mattigod. 1992. Modeling boron adsorption on kaolinite. Clays Clay Miner. 40:192–205.

Sposito, G. 1983. Foundations of surface complexation models of the oxide–aqueous solution interface. J. Colloid Interface Sci. 91: 329–340.

Su, C., and D.L. Suarez. 1995. Coordination of adsorbed boron: A FTIR spectroscopic study. Environ. Sci. Technol. 29:302–311.

Suarez, D.L., and J. Simunek. 1997. UNSATCHEM: Unsaturated water and solute transport model with equilibrium and kinetic chemistry. Soil Sci. Soc. Am. J. 61:1633–1646.

Toner, C.V., and D.L. Sparks. 1995. Chemical relaxation and double

layer model analysis of boron adsorption on alumina. Soil Sci. Soc. Am. J. 59:395–404.
Westall, J., and H. Hohl. 1980. A comparison of electrostatic models for the oxide/solution interface. Adv. Colloid Interface Sci. 12: 265–294.